Applied Clay Science 134 (2016) 83–88

Contents lists available at ScienceDirect

Applied Clay Science

journal homepage: www.elsevier.com/locate/clay

Research paper

Microelectrophoresis and inverse gas chromatography as tools to study the surface interactions between a fluorinated fungicide and raw or organically modified Patagonian montmorillonite

F.M. Flores [a], M. Gamba [a], R.M. Torres Sánchez [a], E. Brendlé [b], J. Brendlé [c,*]

[a] CETMIC-CCT La Plata, CIC, Camino Centenario y 506, 1897 M. B. Gonnet, Argentina
[b] Adscientis, 1 rue A. Kastler, 68310 Wittelsheim, France
[c] Pôle Matériaux à Porosité Contrôlée, Institut de Science des Matériaux de Mulhouse, CNRS-UMR 7361, Université de Haute-Alsace, Université de Strasbourg, 3 rue Alfred Werner, 68093 Mulhouse, France

ARTICLE INFO

Article history:
Received 29 October 2015
Received in revised form 25 February 2016
Accepted 29 February 2016
Available online 9 March 2016

Keywords:
Montmorillonite
Organo-montmorillonite
Inverse gas chromatography
Zeta potential
Surface properties

ABSTRACT

The importance of fungicides uses to maintain healthy crops and reliable, high-quality yields poses environmental issues due to the water and soil contaminations. The montmorillonite is known as efficient adsorbent for many pesticides, while the organo modification enabled to use them in wider range of applications. In this study, the fungicide fludioxonil (FDX) was adsorbed on raw and organo-modified Patagonian montmorillonite. The effects of the organo treatment as well as the FDX adsorption on the surface properties were investigated by X-ray diffraction, microelectrophoresis and inverse gas chromatography. The importance of the organo treatment was revealed both for the changes in the surface properties (dispersive component of the surface energy, nanoroughness and surface acidity as well as zeta-potential) and for the adsorption of FDX as it enabled increase two times respect to the pristine montmorillonite.

© 2016 Elsevier B.V. All rights reserved.

1. Introduction

Fungicides are essential for maintaining healthy crops and reliable, high-quality yields. The fungicides market consists of a specific type of pesticide that controls fungal disease by specifically inhibiting or killing the fungus causing the disease in the crops. They prevent and cure diseases, which can have severe adverse effects on crop yields and quality. The main markets are fruit and vegetables, cereals, and rice. The competition of fungicide industry in key growth regions will be increasingly fierce in coming years as more and more players get into fungicide business.

The regular use of bioactive molecules poses environmental issues including mainly their leaching and migration in soils and groundwater. The migration off-site and entering waterways are due to the spray drift and run-off. If this occurs, it could lead to adverse impacts to the health of terrestrial and aquatic ecosystems. For instance, concerns have been raised over the long term use of copper-based fungicides, which can result in an accumulation of copper in the soil. This in turn can have adverse effects on soil organisms (e.g. earthworms, microorganisms) and potentially pose a risk to the long-term fertility of the soil.

Argentine production of pears, apples and lemons utilized more than 100,000 ha where particularly postharvest fungicides are used to maintain in good conditions the fruits up to attain international markets. Losses of untreated fruit from fungal decay have been estimated to be as high as 90% during postharvest handling and marketing. Due to many citizens use groundwater as drinking water, the leaching of fungicides after agricultural activities generated an environmental and public health concern throughout the world. Thiabendazole and imazalil have been registered for postharvest use against citrus decays for long time ago. Treatment efficacy using these fungicides, however, is often compromised due to the occurrence of resistant pathogen populations.

The reduced efficacy of these fungicides combined with their periodic regulatory review and potential withdrawal or cancellation stimulated the research on new materials that could be effectively incorporated into a postharvest decay control program. Within the potential new fungicides introduced in 2007 to replace thiabendazole is the fludioxonil, which is classified as reduced-risk fungicides by the U.S. Environmental Protection Agency. The EU established the individual (0.1 g L^{-1}) and total (0.5 g L^{-1}) concentrations of pesticides in drinking water to safeguard people from harmful effects. Patagonia montmorillonite will be used in this study since it is an abundant locally natural resource which can be used for industrial processes, and was also proved in previous woks to retain Thiabendazole (Lombardi et al., 2003, 2006). Organo-modified montmorillonite will be prepared starting from

* Corresponding author.
E-mail address: Jocelyne.Brendle@uha.fr (J. Brendlé).

http://dx.doi.org/10.1016/j.clay.2016.02.034
0169-1317/© 2016 Elsevier B.V. All rights reserved.

alkylammonium cations such as octadecyltrimethylammonium cations in order to propen the interlayer space, enabling therefore species to be introduced and enhancing the compatibility between organic species and montmorillonite. Adsorption experiments will be carried out and a deep characterization of the recovered solids by X-ray diffraction, microelectrophoresis and inverse gas chromatography (IGC) will enable gathering information on the importance of the surface properties to retain the fungicide. Inverse gas chromatography is a powerful and versatile method of determining the surface heterogeneity of solids (Saada et al., 1995; Voelkel et al., 2009; Mohammadi-Jam and Waters, 2014; Bilgiç et al., 2014) and delivers the dispersive component of the surface energy, surface charge as well as nanoroughness and acidic-base character. On the contrary of gas chromatography, in inverse gas chromatography, the stationary is analysed and chosen and known molecules, called molecular probe are injected in order to get chromatograms.

IGC methods exist depending on the injected molecular probe amounts. The first one, is called IGC at infinite dilution (ID) because in this case, very low amounts of molecular probes are injected. In such situation, the interactions between the molecular probes are negligible and the retention time is only depending on the interactions occurring with the investigated stationary phase. IGC-ID is applied to characterize the properties of solid surfaces. The second method, is IGC at finite concentration (IGC-FC) and consists in injecting a most important molecular probe amount. Here, the reached surface coverage ratios are close to the monolayer or even higher. This method is applied mainly in gas/solid chromatography with the goal to determine desorption isotherms, specific surface area and measuring the surface heterogeneity. One novelty of the present study stands in the combined use of microelectrophoresis and inverse gas chromatography.

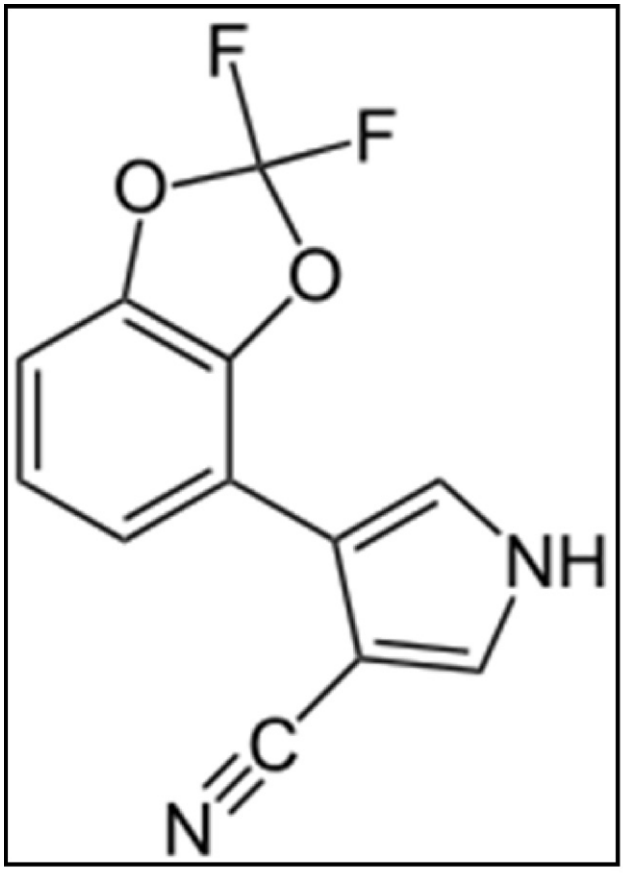

Fig. 1. Molecular structure of fludioxonil.

Table 1
Amount of FDX adsorbed.

Sample	Adsorbed ($mg \cdot g^{-1}$)	Adsorbed (wt%)
MtB-FDX	8.3 ± 0.9	16 ± 2
OMt137B-FDX	21.0 ± 0.8	40 ± 1

2. Experimental

2.1. Materials

The raw montmorillonite (Mt) sample was provided by Castiglioni Pes and Cia. (Lago Pellegrini deposit, Rio Negro, North Patagonia, Argentina) and used as received. In a previous work (Magnoli et al., 2008), the structural formula was obtained from the chemical analysis of purified Mt: $Na^{+}_{0.41}[(Si_{3.89}Al_{0.11})(Al_{1.43}Fe^{3+}_{0.28}Mg_{0.30})O_{10}(OH)_2]$. The isoelectric point (IEP) equals 2.7, the specific surface area (SSA) is 34.0 m^2/g and the total specific surface area (TSSA) equals 621 m^2/g (Magnoli et al., 2008). The cationic exchange capacity (CEC) determined by the Cu-triethylenetetramine method was 0.825 mmol/g clay (Gamba et al., 2015).

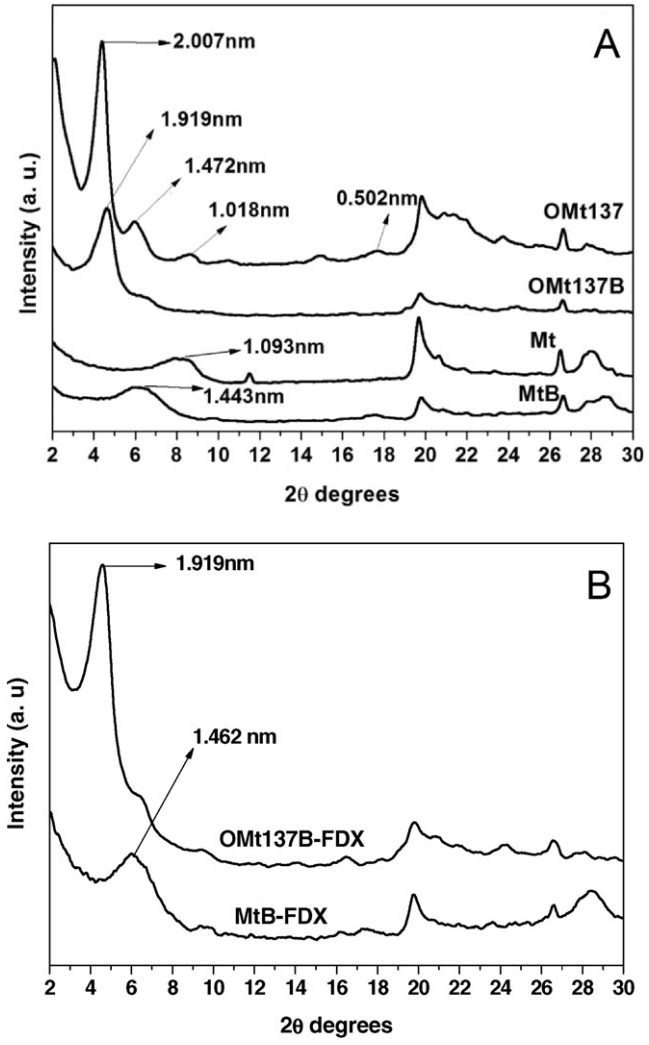

Fig. 2. XRD patterns of: (A) Mt, MtB, OMt137 and OMt137B and (B) MtB-FDX and OMt137B-FDX samples.

Table 2
Measurements of apparent diameter (Dapp) of indicated samples.

Sample	Dapp (nm)
Mt	674 ± 51[a]
MtB	559 ± 16
MtB-FDX	675 ± 26
OMt137	8351 ± 46[a]
OMT137B	2407 ± 218
OMt137B-FDX	2456 ± 156

[a] Data from Gamba et al. (2015).

Fludioxonil (FDX, Fig. 1) PESTANAL®, analytical standard (purity: 99%) was supplied by Fluka-Sigma-Aldrich and used as received. The IUPAC name of FDX is 4-(2,2-difluoro-1,3-benzodioxol-4-yl)-1H-pyrrole-3-carbonitrile, with molecular mass = 248.19 g mol^{-1} and solubility in water 1.8 mg L^{-1} at 25 °C (Komárek et al., 2010). Usually methanol solution was used to obtain a stock standard solution of high FDX concentration (Pose-Juan et al., 2011; Duan et al., 2013; Arias et al., 2005). A methanol/water (50:50) mixture was used in order to increase the solubility of FDX and attain a high initial concentration (close to 200 mg L^{-1}) and 52.2 mg $L^{-1}$was used in the adsorption experiments.

Also, to be used as reference, Mt was contacted with a methanol/water (50:50) solution (1 g L^{-1}) and kept during 24 h with continuous stirring. The solid was then recovered by centrifugation at 15,000 rpm during 15 min and dried at 80 °C (sample MtB).

Octadecyltrimethylammonium (ODTMA) bromide [$C_{18}H_{37}N(CH_3)_3Br$] (≥97%), with molecular mass = 392.5 g mol^{-1}, was from Fluka (Buchs, Switzerland), and used as received. To attain ODTMA-Mt sample correspondent amount of ODTMA-Br was exchanged to obtain 2.11 CEC of Mt using the procedure of previous work (Gamba et al., 2015), the real surfactant loading obtained was 137% CEC (Gamba et al., 2015). The product obtained was labelled as OMt137. Also, to be used as reference, OMt137 was contacted and kept 24 h with methanol/water (50:50) (1 g L^{-1}) with continuous stirring (OMt137B).

2.2. FDX adsorption

The FDX solution was contacted with Mt and OMt137, with an adsorbent/adsorbate ratio of 1 g·L^{-1}, during 24 h, at 20 °C and pH 7.4 under continuous stirring and adsorption were done in duplicate.

After the contact time, the suspensions were centrifuged at 15,000 rpm during 15 min. FDX concentration in the supernatants was analysed by High Performance Liquid Chromatography (HPLC) coupled with UV–Visible detection (λ = 210 nm) using a Shimadzu HPLC C18 column (4.6 mm × 250 mm, 4.6 μm). The mobile phase was 50/50 acetonitrile/water mixture flowing at 1.4 mL min^{-1}, and the injected volume was 20 μL. The amount of adsorbed FDX, Q (mg FDX/g adsorbent) was determined as the difference between the initial FDX concentration (C_o) and that after contact time (C_{eq}). The samples were labelled MtB-FDX and OMt137B-FDX.

2.3. Characterization methods

Powder samples dried at 80 °C overnight were analysed by XRD in the range 2° < 2θ < 30°, with counting time of 10 s/step, 0.02° (2θ) step size, 40 kV and 30 mA with Cu Ka radiation using a Philips PW 1710 diffractometer.

The electrophoretic mobility determination was performed in a microelectrophoresis (Zeta potential function) Brookhaven 90Plus/BiMAS equipment. The electrophoretic mobility values obtained were converted into Zeta potential ones automatically using the Smoluchowski equation (Hunter, 1981). The samples were dispersed (1 g·L^{-1}) in 10^{-3} M KCl solution, used as inert electrolyte, Pd electrodes and the dispersions pH were adjusted adding drops of HCl or KOH of different concentrations followed by magnetic stirring until equilibrium was attained (10 min).

Particle size determinations were achieved using the same Brookhaven equipment utilized for electrophoretic mobility measurements, employing Multi Angle Particle Sizing function and dynamic light scattering (DLS). For each determination, samples were dispersed in 10^{-3} M KCl solution to attain 1% w/w suspensions. The equipment operated at: λ = 635 nm, 15 mW solid state laser, scattering angle = 90°, and temperature = 25 °C. The determination rendered the apparent equivalent sphere diameter, Dapp.

The surface properties of the samples (dispersive component of the surface energy γ^d_s, nanoroughness and acid-base characteristics) were investigated at Adscientis company by Inverse Gas Chromatography (IGC) at infinite dilution (ID) using a Fisons Mega HRGC 2 apparatus with flame ionization detector. Each sample used as chromatographic stationary phase, was introduced in a stainless steel column. All the samples were conditioned at 130 °C over night, using dry He as carrier gas (12 mL·min^{-1}). The measurements were performed at 110 °C, applying a carrier gas flow of around 20 mL·min^{-1}, precisely measured with a digital flow meter (Agilent AMD 1000). On each samples several molecular probes (*n*-alkanes (from C_2 to C_{12})), branched and cyclic alkanes (isooctane and cyclooctane respectively), polar molecules (acetonitrile, acetone, tetrahydrofuran (THF), ether, chloroform, methylacetate, benzene) were injected at infinite dilution conditions (<1 μL). Each molecular probe was injected at least three times and their net retention time was measured ($t_N \pm \Delta t_N$). The measured probe retention times T_N can be treated assuming that only probe-surface interactions occur. With the respect of the infinite dilution conditions, Doris and Gray (1980) proposed that the measured retention times are directly related to their free energy change of adsorption (ΔG°_a) as follows (Eq. (1)):

$$\Delta G^\circ_a(\text{probe}) = -R \cdot T \cdot \ln(V_N) + C \quad (1)$$

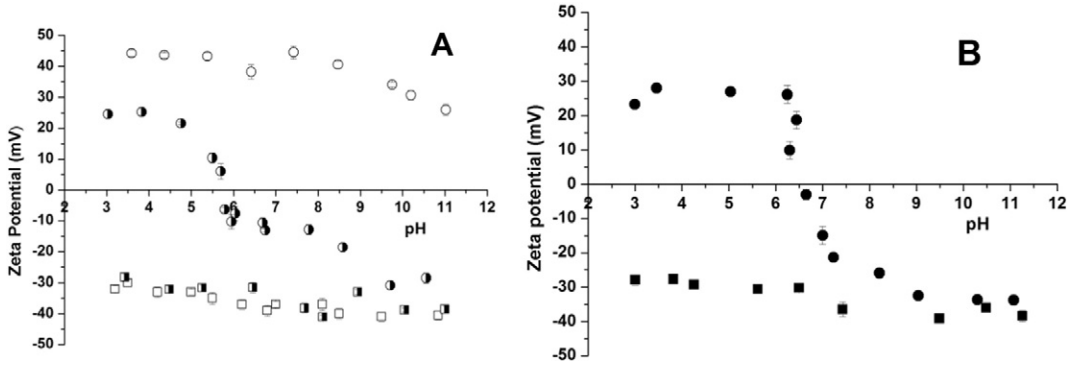

Fig. 3. Zeta potential vs. pH curves for all samples. Symbols indicated: (A) (□) Mt, (■) MtB, (○) OMt137, and (◑) OMt137B samples; (B) (■) MtB-FDX and (●) OMt137B-FDX samples.

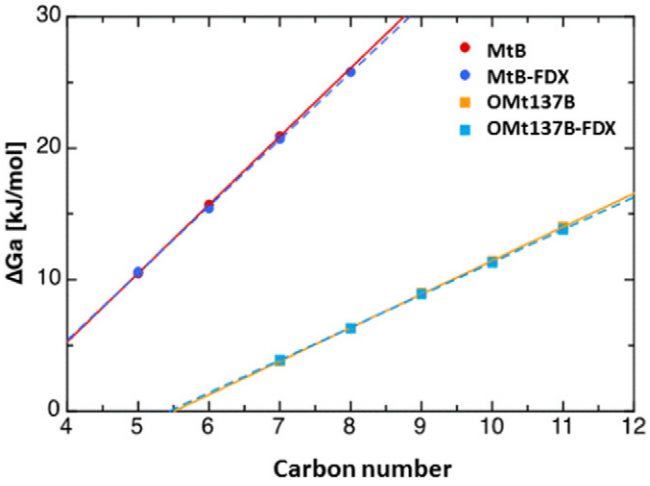

Fig. 4. *n*-Alkane straight lines obtained at 25 °C for samples MtB, MtB-FDX, OMt137B and OMt137B-FDX.

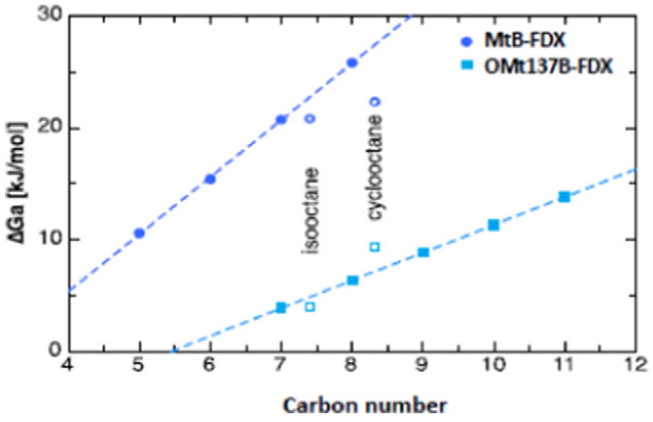

Fig. 5. Behaviour of the branched and cyclic alkane probes versus *n*-alkanes for samples MtB-FDX and OMt137B-FDX.

where T is the measurement temperature, V_N the net retention volume and C a constant depending on a theoretical bi-dimensional reference state for the adsorbed molecules. In order to avoid the use of this reference state, they proposed an approach based on the fact that, for *n*-alkanes, the free energy change of adsorption varies in a linear way with the number of their carbon atoms. With help of this linear behaviour, a free energy increment by methylene group ($\Delta G_a(CH_2)$) is determined that corresponds to the slope of the *n*-alkanes line and is no more depending on C (Eq. (2)).

$$\Delta G_a(CH_2) = R \cdot T \cdot \ln((V_N + 1)/V_N). \quad (2)$$

The *n*-alkane probes are non-polar and only able to exchange non-specific interactions with the surface (London Forces). Therefore, the work of adhesion of the methylene unit to a surface $W^{CH_2}{}_a$, as described by Fowkes (1964), can be written (Eq. (3)):

$$W^{CH_2}{}_a = 2N \cdot a_{CH_2} \cdot \left(\gamma^d{}_s \cdot \gamma_{CH_2}\right)^{1/2} \quad (3)$$

with a_{CH_2} the area of a methylene unit, N the Avogadro's number and γ^{CH_2} the surface energy of a solid made only of methylene units (i.e. polyethylene).

Since the adsorption and the work of adhesion are reversible, it is possible to bring them closer (Eq. (4)):

$$\Delta G_a(CH_2) = W^{CH_2}{}_a. \quad (4)$$

By combining the two last equations, the dispersive component of the surface energy $\gamma^d{}_s$ can be calculated with the following equation (Eq. (5)):

$$\gamma^d{}_s = (\Delta G_a(CH_2))^2 / \gamma^{CH_2} (2N \cdot a_{CH_2})^2. \quad (5)$$

It is worth to underline that this approach supposes that the *n*-alkane probes adsorb flat on the surface and that the surface is homogeneous.

The method of determination of solid's surface morphology is based on the topology index concept of molecules (χT) which takes into account the shape (geometry) of molecules and describe their Van der Waals volume (Brendlé and Papirer, 1997). The morphology index (IM) is given by the ratio of the free enthalpies of adsorption of one branched or cyclic alkane molecule and the free enthalpies of adsorption of an *n*-alkane having the same accessibility to the solid's surface.

The specific interaction parameter (ISP) was determined with reference to the *n*-alkane straight line (Saint Flour and Papirer, 1983). This is achieved by considering that the gap of free energy change of adsorption between the representative point of the polar probe (ΔG_a) and its projection on the alkanes straight line ($\Delta G^d{}_a$), will correspond to the contribution of the specific interactions ($\Delta G^{SP}{}_a$). So the ISP of a probe is given, in kJ/mol, by the following expression (6):

$$ISP = \Delta G^{SP}{}_a = \Delta G_a - \Delta G^d{}_a. \quad (6)$$

3. Results and discussion

3.1. FDX adsorbed on Mt or OMt137samples

Fludioxonil is a neutral molecule over a wide pH range ($pKa_1 = 0$; $pKa_2 = 14.1$) and is low adsorbed on raw montmorillonite (see Table 1) and the Mt is negatively charged at the suspension pH (pH = 7.4), the more positive charged organo-Mt (sample OMt137) was chosen in order to evaluate an adsorbent sample with opposite electric charge respect to Mt. The higher adsorption for FDX on OMt137 than Mt samples (Table 1) was in agreement to that indicated by Sanchez-Martin et al. (2006), for different pesticides and the designated adsorption mechanism was leaded by partition of the organic phase derived by the loaded surfactant.

Table 3
Results of the slope of the *n*-alkane straight lines ($\Delta G_a(CH_2)$) and corresponding surface energy (γ^d_s) determined at 25 °C for samples MtB, MtB-FDX, OMt137B and OMt137B-FDX.

Samples	$\Delta G_a(CH_2)$	γ^d_s [mJ m^{-2}]	r^2
MtB	5.19 ± 0.01	169.9 ± 6.9	1.0000
MtB-FDX	5.09 ± 0.06	163.2 ± 9.7	0.9997
OMt137B	2.55 ± 0.01	41.2 ± 1.9	0.9999
OMt137B-FDX	2.47 ± 0.02	38.5 ± 1.9	0.9999

Table 4
Results of nanoroughness IM index [n.u.] determined at 25 °C on samples MtB, MtB-FDX, OMt137B and OMt137B-FDX.

Samples	IM (isooctane)	IM (cyclooctane)
MtB	0.53 ± 0.02	0.20 ± 0.01
Mt-FDX	0.56 ± 0.02	0.20 ± 0.01
OMt137B	0.76 ± 0.03	1.99 ± 0.09
OMt137B-FDX	0.77 ± 0.05	2.02 ± 0.08

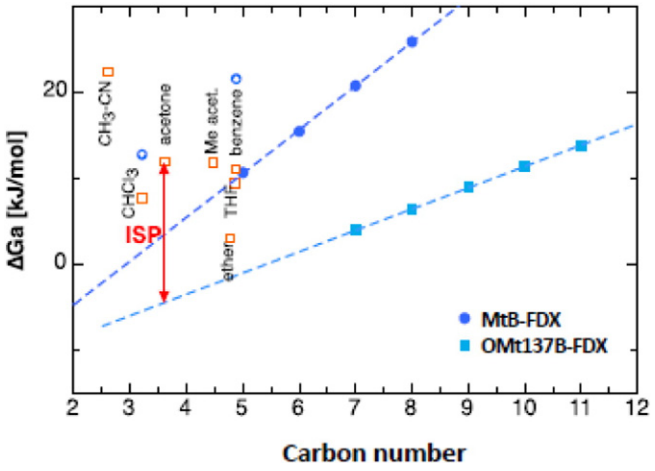

Fig. 6. *n*-Alkanes straight lines and polar probes used for the ISP values determination on samples MtB-FDX and samples OMt137B-FDX.

3.2. Characterization of Mt, OMt137 and FDX adsorbed samples

XRD was utilized for check the shift of 001 reflection for Mt, MtB, OMt137 and OMt137B samples (Fig. 2A), which was indicative of the interlayer variation. The presence of methanol on Mt sample generated a basal space increase from 1.093 to 1.443 nm, confirming the entrance of methanol into the clay interlayer (Amarasinghe et al., 2009; Morozov et al., 2014).

The surfactant loading and interlayer entrance (He et al., 2006) also generated an interlayer space increase, reflected in the d001-value shift from 1.443 to 1.919 nm for MtB and OMt137B samples, respectively.

For OMt137 and OMT137B well-ordered structures were found (Fig. 2A) where a model of pseudo-trilayer arrangement can be inferred (Zhu et al., 2003; Lagaly and Dékany, 2005). A small shift of d001 value was observed from 2.007 to 1.919 nm, for OMt137 and OMt137B samples, respectively, that it could be due to a removal of weakly bound surfactant by methanol in the interlayer (Elban et al., 2012). Also a new peak appeared at 1.472 nm in OMt137B and OMt137 samples originated in multiphase systems consisting of both regularly and randomly intercalated layers (He et al., 2006; Bianchi et al., 2013). In OMt137 sample the 002 and 003-values at 1.018 and 0.502 nm, respectively, were also observed generated from interactions between surfactant alkyl chain-silicate surface and alkyl chain-alkyl chain of the alkyl ammonium cations (Sarkar et al., 2011), while in OMt137B sample the methanol presence could remove weakly bound surfactant in the interlayer (Elban et al., 2012).

The samples MtB-FDX and OMt137B-FDX (Fig. 2B) showed little or no significant modification of the interlayer space, respectively, compared to same samples without FDX, which could be assigned to different behaviour. For MtB-FDX sample a screening effect could be conceivable due to the presence of methanol, in the widening of the interlayer (from 1.443 to 1.462 nm) by FDX adsorption. However for OMt137B-FDX sample, despite the greater amount of FDX adsorbed than in MtB-FDX sample (Table 2), no modification of the basal space was found, that could indicate no entrance of FDX in the surfactant loaded interlayer.

Similar Zeta potential curves were found for Mt and MtB samples, indicating no change of the classical negative structural surface charge of montmorillonite (Bianchi et al., 2013) by the presence of methanol (Fig. 3A), mainly in the interlayer as evidenced XRD analysis (Fig. 2A). However the positive charge of the outer surface attained for OMt137 sample (Gamba et al., 2015, Fig. 3A) was strongly modified by the presence of methanol in OMt137B sample which also showed a well-defined edge's isoelectric point (IEP) at pH 5.7. This last behaviour could be attributed, to a main remotion of weakly bound surfactant, as was evidenced by XRD analysis at the interlayer (Elban et al., 2012), and also at the outer or edge surface of OMt137. Pecini and Avena (2013) indicated an edge's IEP at pH around 5 when Methylene Blue (MB) was adsorbed on Mt sample and also pointed out the important amount of MB released by ethanol washing.

Zeta potential curves for Mt and MtB-FDX samples (Fig. 3A and B) coincided within the experimental error (±0.1 pH) and Zeta potential values were dominated by negative structural charge of the clay mineral (Pecini and Avena, 2013). While the FDX adsorption on OMt137B-FDX sample produced an increase in the edge's IEP from pH = 5.7 to 6.5 (Fig. 3B). This behaviour confirmed that the FDX was adsorbed on the edge variable charges by partition of the organic phase (loaded surfactant).

Dapp values showed a huge increase (Table 2) in aggregate size for OMt137 regarding to Mt samples, in agreement with previously found by Gamba et al. (2015) and for MB by Pecini and Avena (2013), and associated to the surfactant adsorption at the external surface (Janek and Lagaly, 2003). The methanol addition generated decrease in aggregate sizes for Mt sample which can be associated with the entrance of methanol into the clay interlayer (Amarasinghe et al., 2009; Morozov et al., 2014), while for organo montmorillonite, a huge decrease in aggregate size was assigned to the surfactant released by methanol. The same trend was observed after FDX adsorption on both samples.

Inverse Gas Chromatography (IGC) at infinite dilution (ID) was performed in order to follow the evolution of the dispersive component value of the surface energy (γ_s^d) between samples MtB, OMt137B before and after FDX adsorption. The γ_s^d value was determined starting from the slope of the straight line obtained from the plot of the *n*-alkane ΔG_a versus their number of carbon atoms. The Fig. 4 compared the *n*-alkane straight lines obtained on the four samples. It is worthy to note that the straight lines corresponding to samples MtB and MtB-FDX take place above the samples OMt137B and OMt137B-FDX.

The value of the slope of the straight lines, $\Delta G_a(CH_2)$, and the corresponding γ_s^d values were reported on Table 3. The results showed that the organo-treatment of MtB reduced significantly the surface energy values ($\gamma_s^d \approx 170$ mJ m^{-2} for samples MtB and ≈ 41 mJ m^{-2} for samples OMt137B), whereas the FDX adsorption seemed not influence the measured surface energy of the samples. The decrease of the dispersive component of the surface energy value after organo treatment of silica and clays was already mentioned (Papirer et al., 1992; Picard et al., 2007).

The nanoroughness determination was achieved by comparing the behaviour of the *n*-alkane probes with those of branched and cyclic probes. Two probes were injected for that purpose: cyclooctane and isooctane. The behaviour of the linear, cyclic and branched alkanes was displayed on Fig. 5 for samples MtB-FDX and OMt137B-FDX. The branched alkanes were taking place bellow the *n*-alkanes reference straight line for samples MtB-FDX and OMt137B-FDX. In contrast, the cyclic probe (cyclooctane) takes place bellow (sample MtB-FDX) or above (sample OMt137B-FDX). This indicates that dissolution effects occurred for sample OMt137B-FDX, i.e. ODTMA treatment masked the initial surface nanoroughness and was dense enough to lead to probe solubility effects with the C_{18} chains.

The morphology index (IM) value is a description of the importance of the size exclusion effects, i.e. of the surface nanoroughness, or of the

Table 5
Results of the specific interaction (ISP [kJ/mol]) determination at 25 °C.

Sample/probe	MtB	Mt-FDX	OMt137B	OMt137B-FDX
Acetonitrile	Not eluted	Not eluted	31.2 ± 0.4	29.3 ± 0.3
Acetone	Not eluted	Not eluted	17.4 ± 0.2	16.4 ± 0.2
THF	Not eluted	Not eluted	11.3 ± 0.2	10.8 ± 0.1
Ether	Not eluted	Not eluted	4.0 ± 2.3	4.6 ± 1.7
Chloroform	11.9 ± 0.1	11.3 ± 0.3	13.8 ± 0.2	13.0 ± 0.2
Me-acetate	Not eluted	Not eluted	14.8 ± 0.2	14.1 ± 0.2
Benzene	11.6 ± 0.2	11.7 ± 0.3	12.7 ± 0.1	12.3 ± 0.1

dissolution effects. The values of the morphology index (IM) measured for the four samples were reported in Table 4 here above. An IM value of 1 corresponded to zero size exclusion effect, i.e. flat surfaces at the molecular scale. Lower IM values (for all the probes) were indicating stronger size exclusion effects (i.e. nanoroughness). The values obtained for samples MtB and MtB-FDX were similar whatever the probe, the same trend was observed for samples OMt137B and OMt137B-FDX. Whatever the probes, the IM values were below 1 for samples MtB and MtB-FDX, mean that there was a surface nanoroughness. The measured IM values were lower than 1 in the case of isooctane but were above 1 for cyclooctane for samples OMt137B and OMt137B-FDX. This indicated that probe solubility occurred (probe penetrates into the bulk) meaning that not only probe-surface interactions occur but also probe-bulk interactions. Physically, one IM value of 1.99 determined for cyclooctane on sample OMt137B meant that the measured retention time for this probe was 199% of the expected retention time, assuming an identical accessibility to the surface as for the *n*-alkanes. It can be concluded that the organo-treatment leaded to both a decrease of the surface energy and of the nanoroughness and that the adsorption of FDX had no significant effect. This may be due to the low adsorbed amount.

Information on the acid-base character was obtained by using a series of polar probes. Just as for the morphology indexes, the specific interaction parameters (ISP) will be determined with reference to the *n*-alkane straight line. This was achieved by considering that the gap of free energy change of adsorption between the representative point of the polar probe (ΔG_a) and its projection on the alkanes straight line ($\Delta G^d{}_a$), will correspond to the contribution of the specific interactions ($\Delta G^{SP}{}_a$). The measurements involving the polar probes were also performed at 25 °C. Fig. 6 illustrated the behaviour of the polar probes for samples MtB-FDX and samples OMt137-FDX. This figure displayed also the determination method of the specific interaction parameter value ($ISP = \Delta G^{SP}{}_a$) in the case of acetone.

The obtained ISP values [kJ/mol] were given in Table 5.

Only the most acidic probes were eluted ($CHCl_3$ and benzene) on samples MtB and MtB-FDX. All the basic and amphoteric probes were not eluted. This is explained by the strong surface acidity (Lewis type). On the opposite, all the probes were eluted on samples OMt137 and OMt137-FDX meaning that the organo-treatment shields the surface acidity of the Mt.

4. Conclusions

The treatment of the raw Patagonian Mt with ODTMA led to an increase of the interlayer space from 1.09 to 2.1 nm. It is worthy to note that this treatment greatly affected the surface properties of the Mt as nicely showed by inverse gas chromatography. Indeed the dispersive component of the surface energy strongly decreased as well as the nanoroughness and the surface acidity. The low adsorption of FDX on Mt did not change significantly the initial electric surface charge nor the aggregate size, whereas for organo montmorillonite an increase of the edge's IEP was observed and also a huge decrease of the aggregate size. This study underlined the importance of organo-modification on the FDX adsorption. Further experiments by ^{19}F and ^{13}C solid state NMR will provide insight on the interactions between the solid surface and FDX.

Acknowledgments

The authors acknowledge financial help from Ministerio de Ciencia y Técnica, Agencia Nacional de Promoción Científica y Tecnológica, MINCyT-ANPCyT-FONCyT through PICT/2014-0585, and through FONARSEC FSNano-008 FSNano-008. R.M.T.S. is a member of CONICET and F.M.F. and M.G. acknowledge CONICET fellowships.

References

Amarasinghe, P.M., Katti, K.S., Katti, D.R., 2009. Nature of organic fluid–montmorillonite interactions: an FTIR spectroscopic study. J. Colloid Interface Sci. 337, 97–105.
Arias, M., Torrente, A.C., López, E., Soto, B., Simal-Gándara, J., 2005. Adsorption–desorption dynamics of cyprodinil and fludioxonil in vineyard soils. J. Agric. Food Chem. 53, 5675–5681.
Bianchi, A.E., Fernández, M., Pantanetti, M., Viña, R., Torriani, I., Torres Sánchez, R.M., Punte, G., 2013. ODTMA$^+$ and HDTMA$^+$ organo-montmorillonites characterization: new insight byWAXS, SAXS and surface charge. Appl. Clay Sci. 83-84, 280–285.
Bilgiç, C., Topaloğlu Yazıcı, D., Karakehya, N., Çetinkaya, H., Singh, A., Chehimi, M., 2014. Surface and interface physicochemical aspects of intercalated organo-bentonite. Int. J. Adhes. Adhes. 50, 204–210.
Brendlé, E., Papirer, E., 1997. A new topological index for molecular probes used in inverse gas chromatography for the surface nanorugosity evaluation. J. Colloid Interface Sci. 194, 207–216.
Doris, G.M., Gray, D.G., 1980. Adsorption of n-alcane at zero coverage on cellulose paper and wood fibers. J. Colloid Interface Sci. 77, 353–362.
Duan, Y., Ge, C., Liu, S., Chen, C., Zhou, M., 2013. Effect of phenylpyrrole fungicide fludioxonil on morphological and physiological characteristics of *Sclerotinia sclerotiorum*. Pestic. Biochem. Physiol. 106, 61–67.
Elban, W., Howarter, J., Richardson, M., Stutzman, P., Forster, A., Nolte, A., Holmes, G., 2012. Influence of solvent washing on interlayer structure of alkylammonium montmorillonites. Appl. Clay Sci. 61, 29–36.
Fowkes, F.M., 1964. Attractive forces at interfaces. Ind. Eng. Chem. Chem. 56, 40–52.
Gamba, M., Flores, F.M., Madejová, J., Torres Sánchez, R.M., 2015. Comparison of imazalil removal onto montmorillonite and nanomontmorillonite and adsorption surface sites involved: an approach for agricultural wastewater treatment some aspects of the adsorption of the fungicide imazalil onto octadecyltrimethylammonium. Ind. Eng. Chem. Res. 54, 1529–1538.
He, H., Frost, R.L., Bostrom, T., Yuan, P., Duong, L., Yang, D., Xi, Y., Kloprogge, J.T., 2006. Changes in the morphology of organoclays with HDTMA$^+$ surfactant loading. Appl. Clay Sci. 31, 262–271.
Hunter, R.J., 1981. Zeta Potential in Colloid Science. Academic Press, New York.
Janek, M., Lagaly, G., 2003. Interaction of a cationic surfactant with bentonite: a colloid chemistry study. Colloid Polym. Sci. 281, 293–301.
Komárek, M., Čadková, E., Chrastný, V., Bordas, F., Bollinger, J.C., 2010. Contamination of vineyard soils with fungicides: a review of environmental and toxicological aspects. Environ. Int. 36, 138–151.
Lagaly, G., Dékany, I., 2005. Adsorption on hydrophobized surfaces: clusters and self-organization. Adv. Colloid Interf. Sci. 114-115, 189–204.
Lombardi, B.M., Baschini, M., Torres Sánchez, R.M., 2003. Optimization of parameters and adsorption mechanism of thiabendazole fungicide by a montmorillonite of North Patagonia, Argentina. Appl. Clay Sci. 24, 43–50.
Lombardi, B.M., Torres Sánchez, R.M., Eloy, P., Genet, M., 2006. Interaction of thiabendazole and benzimidazole with montmorillonite. Appl. Clay Sci. 33, 59–65.
Magnoli, A.P., Tallone, L., Rosa, C.A.R., Dalcero, A.M., Chiacchiera, S.M., Torres Sánchez, R.M., 2008. Commercial bentonites as detoxifier of broiler feed contaminated with aflatoxin. Appl. Clay Sci. 40, 63–71.
Mohammadi-Jam, S., Waters, K.E., 2014. Inverse gas chromatography applications: a review. Adv. Colloid Interf. Sci. 212, 21–44.
Morozov, G., Breus, V., Nekludov, S., Breus, I., 2014. Sorption of volatile organic compounds and their mixtures onmontmorillonite at different humidity. Colloids Surf. A 454, 159–171.
Papirer, E., Balard, H., Sidqi, M., 1992. The grafting of perfluorinated silanes onto the surface of silica: characterization by inverse gas chromatography. J. Colloid Interface Sci. 159 (1), 238–242.
Pecini, E.M., Avena, M.J., 2013. Measuring the Isoelectric Point of the edges of clay mineral particles: the case of montmorillonite. Langmuir 29, 14926–14934.
Picard, E., Gauthier, H., Gérard, J.-F., Espuche, E., 2007. Influence of the intercalated cations on the surface energy of montmorillonites: consequences for the morphology and gas barrier properties of polyethylene/montmorillonites nanocomposites. J. Colloid Interface Sci. 93 (307), 364–376.
Pose-Juan, E., Rial-Otero, R., Paradelo, M., López-Periago, J.E., 2011. Influence of the adjuvants in a commercial formulation of the fungicide "Switch" on the adsorption of their active ingredients: cyprodinil and fludioxonil, on soils devoted to vineyard. J. Hazard. Mater. 193, 288–295.
Saada, A., Papirer, E., Balard, H., Siffert, B., 1995. Determination of the surface properties of illites and kaolinites by inverse gas chromatography. J. Colloid Interface Sci. 175 (1), 212–218.
Saint Flour, C., Papirer, E., 1983. Gas–solid chromatography: a quick method of estimating surface free energy variations induced by the treatment of short glass fibers. J. Colloid Interface Sci. 91 (1), 69–75.
Sanchez-Martin, M.J., Rodriguez-Cruz, M.S., Andrades, M.S., Sanchez-Camazano, M., 2006. Efficiency of different clay minerals modified with a cationic surfactant in the adsorption of pesticides: influence of clay type and pesticide hydrophobicity. Appl. Clay Sci. 31, 216–228.
Sarkar, B., Megharaja, M., Xia, Y., Naidu, R., 2011. Structural characterisation of Arquad® 2HT-75 organobentonites: surface charge characteristics and environmental application. J. Hazard. Mater. 195, 155–161.
Voelkel, A., Strzemiecka, B., Adamska, K., Milczewska, K., 2009. Inverse gas chromatography as a source of physiochemical data. J. Chromatogr. A 1216 (10), 1551–1566.
Zhu, J., He, H., Guo, J., Yang, D., Xie, X., 2003. Arrangement models of alkylammonium cations in the interlayer of HDTMA$^+$ pillared montmorillonites. Chin. Sci. Bull. 48, 368–372.